APERTURE AND CELL SIZE EFFECTS ON SHUNT IMPEDANCE OF ALTERNATING PERIODIC STRUCTURES*

D. Carter
San Jose State College
San Jose, California

and

T. Nishikawa
University of Tokyo
Tokyo, Japan

Introduction

Recent work[1] has shown that significant advantages are obtained in linear acceleration of protons by using an alternating periodic structure (hereinafter referred to as APS) operated in a $\pi/2$ resonant mode. Compared to an equivalent uniform periodic structure (hereinafter referred to as UPS) operated, for maximum shunt impedance, in its resonant π mode, the APS in a $\pi/2$ mode enjoys great advantages in relative immunity from beam loading and detuning effects. It has been shown[2] that, while such advantages (which depend mainly on the frequency separation between the operating and adjacent resonant modes) are attributable only to the difference in the operating mode, shifting operation from the π to the $\pi/2$ mode in a UPS would involve a price of significantly lowered shunt impedance. The APS, on the other hand, obtains such advantages of increased stability while sacrificing little in shunt impedance because of an improved transit time factor attributable to the structure. In fact, an approximate calculation[3] predicted that the shunt impedance of an APS in a $\pi/2$ mode might actually be better than that of a UPS in its π mode.

The calculation of shunt impedance referred to above was based on a weak coupling approximation, which in effect neglected all field variation in the vicinity of the coupling aperture. At best, such an approximation could show only the variation of shunt impedance with cell length ratio and phase velocity, without providing any information on the effect of varying the coupling aperture size. Aperture variation will not only affect shunt impedance and transit time factor directly through the changes it produces in field distribution, but it can also be expected to change the functional dependence of these quantities on cell length ratio. Since experimental data are available for different center bore hole sizes and because of the analytic simplification involved, we will limit the aperture variations considered to variations of bore hole radii.

Field Approximation

To find the dependence of shunt impedance on both cell length ratio and coupling aperture size, it suffices to find an appropriate approximation for the field distribution along the axis. For this purpose we use a scheme similar to that described by Slater[4] to resolve the field around the aperture into symmetric and antisymmetric parts. For the lowest passband, the antisymmetric part is furnished by the TM_{010} mode of each resonant cell, which is essentially a constant value of axial field denoted, E_z^a . The symmetric component, denoted E_z^s , is then calculated to satisfy boundary conditions at the coupling hole. This is done by an appropriate conformal transformation and the result given by Slater,[5] with the origin centered in the coupling hole of radius, a , is:

$$E_z^s = -\nabla\varphi \; ; \quad \varphi = -\frac{2}{\pi} E_o z \left(\tan^{-1} \sqrt{w} + \frac{1}{\sqrt{w}} \right) ,$$

where

$$w = \frac{x^2 + y^2 + z^2 - a^2}{2a^2} + \sqrt{\left(\frac{x^2 + y^2 + z^2 - a^2}{2a^2} \right)^2 + \frac{z^2}{a^2}} \; .$$

Such resolution into symmetric and antisymmetric components is similar to the original treatment of these problems by Bethe[6] and later treatments like Bevensee's.[7] The TM_{010}-mode antisymmetric component corresponds to Bethe's incident field $(\vec{E}_0)$, or Bevensee's short circuit mode (E_0), and the symmetric part corresponds to Bethe's diffracted and reflected fields ($\vec{E}_2$ and $\vec{E}_1$) or Bevensee's open circuit mode (e_1).

For our purposes, as mentioned previously, we are interested in the field on the axis. The symmetric component, E_z^s , reduces on axis $(x = y = 0)$ to:

$$E_z^s(z') = \frac{2E_o}{\pi} \left[\tan^{-1} \frac{z'}{a} + \frac{z'/a}{1 + (z'/a)^2} \right] .$$

It is readily seen that this field is symmetric about the aperture $(z' = 0)$, has no axial component in the plane of the aperture, and approaches a constant field pointing towards (or away from) the aperture on both sides as we move away from the aperture.

The linear combination of the symmetric and antisymmetric modes provides us with solutions satisfying boundary conditions at the coupling aperture. We may now choose the relative amplitude of each component to satisfy other conditions depending on the mode of operation. For a $\pi/2$ mode, we require that $E_z = E_z^a + E_z^s$ shall vanish at the

*Work performed under the auspices of the U.S. Atomic Energy Commission while at Brookhaven National Laboratory, Upton, L.I., New York.

center of one of the cells. Choosing that $\pi/2$ mode, in an APS with long cell length L_1 and short cell length L_2, which has vanishing field at the center of the shorter cell ($z' = L_2/2$), then requires that the constant antisymmetric component should cancel the symmetric component evaluated at $z' = L_2/2$. This condition, $E_z^a = - E_z^s(L_2/2)$, allows us to express the axial field in terms of the above-defined symmetric component alone as:

$$E_z(z') = - E_z^s\left(\frac{L_2}{2}\right) + E_z^s(z') \ .$$

Considerable analytic simplification is introduced without losing any essential information relating to the effect produced by aperture variations if we replace this axial E_z by an exponential function having the same behavior both near the plane of the aperture and far from it. Thus, consistent with the approximate analysis above, an excellent representation for the symmetric component of the axial field is:

$$E_z^s(z') \simeq \pm E_0\left(1 - e^{-4|z'|/(\pi a)}\right) .$$

This can be seen to have the same value $[E_z^s(0) = 0]$ and slope

$$\left.\frac{\partial E_z}{\partial z}\right|_{z=0} = \frac{4E_0}{\pi a}$$

at the aperture as the original approximation above, and it also approaches the same value (E_0) far from the aperture. Now adding that level of constant antisymmetric component required to make the total axial field vanish at the center of the smaller cell, and shifting the origin of the z coordinate to the center of the longer cell ($z = z' + L_1/2$) we obtain the following expression for the total field on the axis:

$$\frac{E_z}{E_0} = \begin{cases} 2 - e^{-2L_2/(\pi a)} - e^{-2L_1/(\pi a)}\, e^{4z/(\pi a)} & \text{for } 0 \le z \le L_1/2 \\[1ex] e^{2L_1/(\pi a)}\, e^{-4z/(\pi a)} - e^{-2L_2/(\pi a)} & \text{for } L_1/2 \le z \le (L_1 + L_2)/2 \ . \end{cases}$$

Since we are interested in comparing shunt impedance for different modes in varying structures, care must be exercised to make such comparisons at constant particle velocity ($v = \beta c$) and constant excitation level. The latter requirement means that we must normalize the field expressions to provide a constant value at the center of the long cavity (i.e., $E_z(0)$ should be independent of L_1, L_2 and a), which in turn makes E_0 depend on these structure parameters. The former requirement (constant β) means that we must keep the repeat length or guide wavelength constant, which in turn removes the independence of L_1 and L_2, i.e., $L_1 + L_2 = \beta\lambda/2$. Imposing these conditions leads to the following modification of the expressions for the axial field:

$$E_z = \begin{cases} \dfrac{2 - e^{-2L_2/(\pi a)} - e^{(\beta\lambda - 2L_2)/(\pi a)}\, e^{4z/(\pi a)}}{2 - e^{-2L_2/(\pi a)} - e^{-(\beta\lambda - 2L_2)/(\pi a)}} & \text{for } 0 \le z \le (\beta\lambda - 2L_2)/4 \\[2ex] \dfrac{e^{(\beta\lambda - 2L_2)/(\pi a)}\, e^{-4z/(\pi a)} - e^{-2L_2/(\pi a)}}{2 - e^{-2L_2/(\pi a)} - e^{-(\beta\lambda - 2L_2)/(\pi a)}} & \text{for } (\beta\lambda - 2L_2)/4 \le z \le \beta\lambda/4 \end{cases}$$

To provide an estimate of the accuracy involved, these expressions may be compared to measured field distributions.[8] One such comparison is shown in Figure 1, where the two curves — one experimental and the other calculated from the approximate theory above — are seen to coincide well within experimental accuracy.

It should be noted that the present choice of origin makes the axial field an even function around $z = 0$, $\mathcal{L}/2$ and $\mathcal{L}$, where $\mathcal{L}$ is the repeat length in all normal modes. It also makes $E_z(z)$ an odd function about $z = \lambda_g/4$ in both the $\pi/2$ mode (where $\mathcal{L} = \lambda_g = \beta\lambda = 2L_1 + 2L_2$) and in the UPS π mode (where $\mathcal{L} = \lambda_g = 2L$). Furthermore, the above expressions for the axial field in the APS $\pi/2$ mode degenerate to $E_z(z)$ in the UPS π mode as both L_2 approaches zero and L_1 approaches L.

Specific Energy Gain

Proceeding to the calculation of shunt impedance, or transit time factor, we first use E_z above to evaluate the specific energy gain (i.e., the energy increase per unit length and charge, $\Delta W/e\mathcal{L}$) for a zero phase synchronous particle ($\omega t = 2\pi z/\lambda_g = 2\pi z/\beta\lambda$) in a repeat length of either $\pi/2$ or UPS π mode.

$$\frac{\Delta W}{e\mathcal{L}} = \frac{1}{\mathcal{L}}\int_0^{\mathcal{L}} E_z(z)\cos\omega t\, dz = \frac{1}{\lambda_g}\int_0^{\lambda_g} E_z(z)\cos\frac{2\pi z}{\lambda_g}\, dz$$

$$= \frac{4}{\lambda_g}\int_0^{\lambda_g/4} E_z(z)\cos\frac{2\pi z}{\lambda_g}\, dz \ ,$$

the last step following from the fact that the product in the integrand is even about $z = \lambda_g/4$. It is again worth noting that the expression above for $(\Delta W/e\mathcal{L})_{\pi/2}$ degenerates to $(\Delta W/e\mathcal{L})_{UPS,\pi}$ as both L_2 vanishes and L_1 approaches L. Performing the integration and simplifying leads to

$$\left(\frac{\Delta W}{e\mathcal{L}}\right)_{\pi/2} =$$

$$\frac{\frac{2}{\pi}\left[2\cos\left(\frac{\pi L_2/a}{\beta\lambda/a}\right) - e^{2L_2/(\pi a)}\right] + \frac{\pi a}{\beta\lambda}\, e^{-(\beta\lambda - 2L_2)/(\pi a)}}{\left[2 - e^{-2L_2/(\pi a)} - e^{-(\beta\lambda - 2L_2)/(\pi a)}\right]\left[1 + \left(\frac{\pi^2 a}{2\beta\lambda}\right)^2\right]}$$

which degenerates to

$$\left(\frac{\Delta W}{e\mathcal{L}}\right)_{UPS,\pi} = \frac{\frac{2}{\pi} + \frac{\pi a}{\beta\lambda}\quad e^{-\beta\lambda/(\pi a)}}{\left[1 - e^{-\beta\lambda/(\pi a)}\right]\left[1 + \left(\frac{\pi^2 a}{2\beta\lambda}\right)^2\right]} .$$

As one of the two factors determining relative shunt impedance per unit length

$$[r_{sh} = (\Delta W/e\mathcal{L})^2 / (P/\mathcal{L})] ,$$

it will be informative to examine the dependence on structure parameters of the square of the ratio of the specific energy gain between the two modes. Defining this latter quantity as relative specific energy gain squared, G_r , we obtain

$$G_r \equiv \frac{(\Delta W/e\mathcal{L})^2_{\pi/2}}{(\Delta W/e\mathcal{L})^2_{UPS,\pi}} =$$

$$\frac{\left[2\cos(\pi F/4) - e^{-FB/2} + \pi e^{-(2-F)B/2}/(2B)\right]^2\left[1 - e^{-B}\right]^2}{\left[1 + \pi e^{-B}/(2B)\right]^2\left[2 - e^{-FB/2} - e^{-(2-F)B/2}\right]^2}$$

where

$$B \equiv \frac{\beta\lambda}{\pi a} \quad \text{and} \quad F \equiv 4L_2/\beta\lambda .$$

Its variation with F (which is in effect a measure of the cell length ratio) and $a/\beta\lambda$ (which measures the effect of bore hole radius) is shown in Fig. 2. Since F = 1 corresponds to a $\pi/2$ mode in a UPS and F = 0 corresponds to a π mode in a UPS, Fig. 2 reveals the characteristic decrease of specific energy gain and relative disadvantage of the $\pi/2$ mode in a UPS structure. Now, however, Fig. 2 reveals that $\pi/2$-mode operation in an APS with $F < 1$ tends to reduce that relative disadvantage. We see also that increasing bore hole radius will likewise increase the relative specific energy gain.

Transit Time Factor

The above-mentioned relative disadvantage of the $\pi/2$ mode in a UPS is, of course, due to the relatively smaller average axial field of the $\pi/2$ mode. If we cancel that effect by normalizing to the average electric field, we obtain the transit time factor, T :

$$T \equiv (\Delta W/e\mathcal{L}) / \overline{|E_0|}$$

where

$$\overline{|E_0|} \equiv \frac{1}{\mathcal{L}} \int_0^{\mathcal{L}} |E_z|\, dz .$$

Using our previously developed expression for E_z in the integral, and noting again that the APS $\pi/2$ mode degenerates to the UPS π mode in the limit of F = 0, we obtain

$$\frac{\overline{|E_0|}_{UPS,\pi}}{\overline{|E_0|}_{\pi/2}} =$$

$$\frac{\left[B - (1 - e^{-B})\right]\left[2 - e^{-FB/2} - e^{-(2-F)B/2}\right]}{\left(1 - e^{-B}\right)\left|B\left(2 - F - e^{-FB/2}\right) - e^{-FB/2} + e^{-(2-F)B/2}\right|} .$$

Multiplying this ratio by $\sqrt{G_r}$ then gives the relative transit time factor, $T_{\pi/2}/T_{UPS,\pi}$, the variation of which is shown in Fig. 3. Here we see the advantage in transit time factor of the $\pi/2$ mode because of better utilization of average axial field. Again we observe that this advantage is increased with increasing F and decreasing bore hole radius, a .

Shunt Impedance

Finally, the calculation of shunt impedance requires an evaluation of the average power loss per unit length, $P/\mathcal{L}$. There are two very simple approximations for this factor to provide mainly qualitative results. Firstly, one may assume the average power loss per unit length as roughly proportional to the square of the axial field. This might apply for strong cell-to-cell coupling where the losses are mainly in the outer cylinder. For such an approximation, $P/\mathcal{L} \propto |E_0|^2$, the shunt resistance per unit length becomes proportional to the square of the transit time factor,

$$r = (\Delta W/e\mathcal{L})^2 / P/\mathcal{L} \propto T^2 ,$$

and the variation of the square root of relative shunt resistance would be similar to that shown in Fig. 3. Alternatively, we may assume the losses are roughly the same as for uncoupled cavities to provide an approximation for the weak coupling case. This might also serve for investigation of variations, such as bore hole radius, which significantly affect only the accelerating field while changing only slightly the total coupling and fields at the cell walls. In the weak coupling approximation, following Beringer, we would set

$$P/\mathcal{L} \propto [1 + (2.405/\pi\beta) - F/2]$$

to obtain a relative shunt resistance

$$\frac{r_{\pi/2}}{r_{UPS,\pi}} = G_r \frac{1 + 2.405/\pi\beta}{1 + (2.405/\pi\beta) - F/2} .$$

The increase of the relative power loss factor multiplying G_r , as F increases from 0, will raise the relative shunt resistance above unity, even for very small bore hole radii. Again there is a range of F where we obtain higher shunt resistance in the $\pi/2$ mode than in the π mode, with results identical to Beringer's in the case of vanishing bore hole radius. The effects in increasing bore hole radius are the same as described previously for the factor G_r and displayed in Fig. 2. This will also result in increasing the range of F in which shunt resistance of an APS $\pi/2$ mode will exceed that of a UPS π mode, as shown in Fig. 4.

In order to remove any possible source of confusion on the effect of varying bore hole radius in a given mode and structure we have plotted the variation of specific energy gain versus bore hole radius, a , with cell length ratio, F , as parameter in Fig. 5. Here we note that the specific energy gain in the π/2 mode decreases with increasing bore hole radius, the decrease being sharp only in the range of small F and small a . The fact that specific energy gain falls with increasing (a) while relative specific energy gain rises with increasing (a) (as indicated in Fig. 2) means only that increasing bore hole radius has a greater effect on the UPS π mode than it does on the APS π/2 mode.

Acknowledgment

The authors would like to thank Professor R.L. Gluckstern, Dr. D. Robertson and Mr. S. Giordano for their helpful discussions.

References

1. S. Giordano, "Some New Radio Frequency Accelerating Structures," IEEE Transactions on Nuclear Science, NS-12, No. 3, 213 (1965); T. Nishikawa, "Normal Mode Analysis of Standing Wave Linacs — Field Excitation and Beam Loading in Linac Cavities," BNL Accelerator Dept. Internal Report AADD-87, November 15, 1965; T. Nishikawa, S. Giordano, and D. Carter, "Dispersion Relation and Frequency Characteristics of Alternating Periodic Structure for Linear Accelerators," BNL Accelerator Dept. Internal Report AADD-88, August 23, 1965.

2. T. Nishikawa, S. Giordano, and D. Carter, loc. cit. pp. 18-19.

3. R. Beringer, "Shunt Resistance of Iris-Loaded Waveguides on the Loose-Coupling Model," BNL Accelerator Dept. Internal Report AADD-76, April 2, 1965.

4. J.C. Slater, "Microwave Electronics," p. 112, D. Van Nostrand, New York, 1950.

5. Ibid., p. 130.

6. H.A. Bethe, "Theory of Diffraction by Small Holes," Phys. Rev. 66, No. 7, 163 (1944).

7. R.M. Bevensee, "Electromagnetic Slow Wave Systems," John Wiley & Sons, New York, 1964.

8. S. Giordano and J. Hannwacker, private communication.

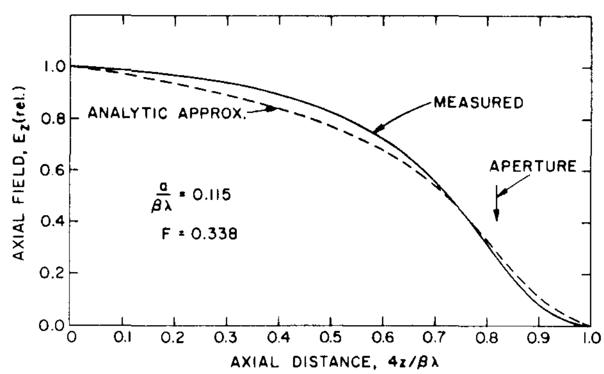

Fig. 1. Axial variation of accelerating fields.

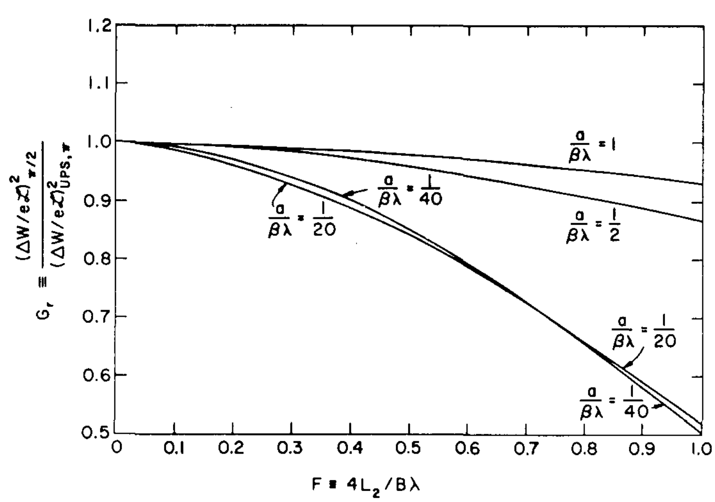

Fig. 2. Relative specific energy gain variation with cell-length ratio: Parameter: bore-hole radius.

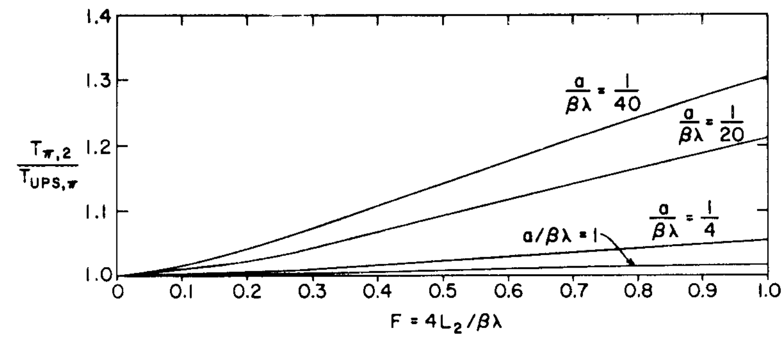

Fig. 3. Transit time factor variation with cell-length ratio. Parameter: bore-hole radius, a.

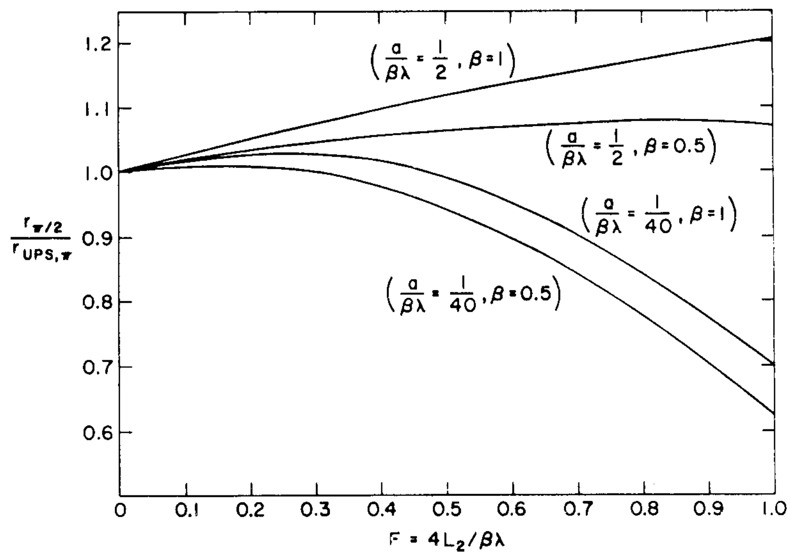

Fig. 4. Relative shunt resistance vs cell-length ratio for weak coupling. Parameters: bore-hole radius and velocity.

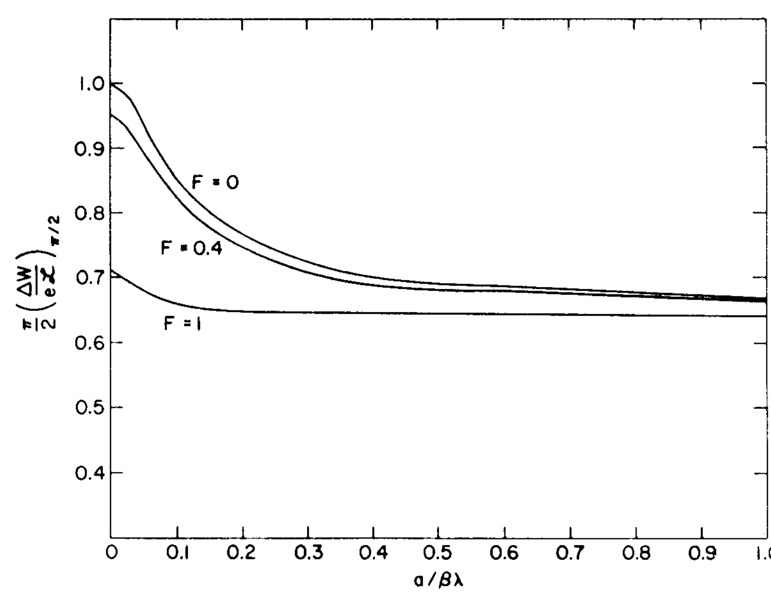

Fig. 5. Specific energy gain vs bore-hole radius. Parameter: cell-length ratio.